Self-Assembly

DOI: 10.1002/ange.200503040

Predictions, Synthetic Strategy, and Isolation of a Linear Tetrametallic Triple-Stranded Lanthanide Helicate**

Kornelia Zeckert, Josef Hamacek, Jean-Michel Senegas, Natalia Dalla-Favera, Sébastien Floquet, Gérald Bernardinelli, and Claude Piguet**

Dedicated to Professor Jean-Claude G. Bünzli

The majority of self-assembled linear multi-stranded helicates are bimetallic, with some extensions toward trimetallic analogues,[1] whilst those with four or more metal centers remain rare.[2] Although the regular arrangement of several metal ions in a single direction, thus forming a discrete chain, may induce novel and unusual electrochemical,[3] photophys-

[*] Dr. G. Bernardinelli
Laboratory of X-ray Crystallography
University of Geneva
24 Quai E. Ansermet, 1211 Geneva 4 (Switzerland)
Fax: (+41) 22-379-6108
E-mail: gerald.bernardinelli@cryst.unige.ch

Dr. K. Zeckert,[+] Dr. J. Hamacek, Dr. J.-M. Senegas, N. Dalla-Favera, Dr. S. Floquet,[++] Prof. Dr. C. Piguet
Department of Inorganic
Analytical and Applied Chemistry
University of Geneva
30 Quai E. Ansermet, 1211 Geneva 4 (Switzerland)
Fax: (+41) 22-379-6830
E-mail: claude.piguet@chiam.unige.ch

[+] Present address: Institut für Anorganische Chemie
der Universität Leipzig
Johannisallee 29, 04103 Leipzig (Germany)

[++] Present address: Institut Lavoisier, IREM, UMR 8637
Université de Versailles
45 Avenue des Etats-Unis, 78035 Versailles (France)

[**] This work was supported through grants from the Swiss National Science Foundation.

Supporting information for this article is available on the WWW under http://www.angewandte.org or from the author.

ical,[4] or magnetic[5] properties, multimetallic linear helicates have been mainly investigated for their structural aspect, which is indebted to their undeniable aesthetic appeal. The recent expansion of (supra)molecular chemistry toward the nanosciences dramatically revealed the very limited quantitative predictions available for the design of large multicomponent assemblies,[6] despite the remarkable reports of major successes based on qualitative symmetry matching and stereochemical restrictions.[7] In this context, the assembly of simple mono-dimensional multimetallic helicates can bring some valuable contributions to the fundamental understanding and rationalization of thermodynamically driven multicomponent complexation processes. In two seminal reports,[8] Lehn and co-workers first proposed a thermodynamic model that accounted for the formation of trimetallic double-stranded helicates. Scatchard plots based on the classical two-parameter site-binding model,[9–11] which considers the total free energy of formation of the final complex as the sum of the connection energies of each metal ion to a single receptor modulated by intermetallic pair interactions, suggested the occurrence of thermodynamic complexation processes driven to completion by positive cooperativity—a landmark that deeply influenced the rationalization of metallosupramolecular self-assembly processes for more than a decade.[10] The recent reanalysis of these original data by Ercolani indicates that helicate formation cannot be modeled with pure intermolecular interactions and entropic corrections must be considered for adequately rationalizing intramolecular metal–ligand connections, which occur during the self-assembly processes.[11] An explicit treatment, which combines metal–ligand connections (intra- and intermolecular) and pair interactions (intermetallic and interligand) has been recently proposed, and the macroscopic formation constant $\beta_{m,n}^{M,L}$ of any supramolecular complex $[M_mL_n]$ [Eq. (1)] can be modeled with four microscopic parameters [Eq. (2), extended site-binding model]:[12]

$$m\,M + n\,L \rightleftharpoons [M_mL_n]\ \beta_{m,n}^{M,L} \quad (1)$$

$$\beta_{m,n}^{M,L} = \sigma_{chir}^{M,L}\,\omega_{m,n} \prod_{i=1}^{mn} (f_i^{M,L}) \prod_{i=1}^{mn-m-n+1} (c_i^{eff}) \prod_{i<j}{}'' (u_{ij}^{MM}) \prod_{k<l}{}''' (u_{kl}^{LL}) \quad (2)$$

1) $f_i^{M,L}$ represents the intermolecular microscopic affinity constant that characterizes the connection of a metal M to the binding site i of a ligand L (including desolvation); 2) $u_{ij}^{MM} = \exp(-\Delta E_{ij}^{MM}/RT)$ is the Boltzman factor that accounts for the intermetallic interaction ΔE_{ij}^{MM} (in terms of free energy), which occurs when two metal centers occupy two adjacent binding sites i and j of the same ligand; 3) $u_{kl}^{LL} = \exp(-\Delta E_{kl}^{LL}/RT)$ is the Boltzman factor that accounts for the interligand interactions ΔE_{kl}^{LL}, which results from the connection of two binding sites k and l to the same metal center; 4) $c_i^{eff} = \exp((\Delta S_{i,intra}^{M,L} - \Delta S_{i,inter}^{M,L})/R)$ is the "effective concentration" used for the correction of the entropy change observed between inter- and intramolecular binding processes; 5) the term $\sigma_{chir}^{M,L}\omega_{m,n}$ represents the degeneracy of the microscopic state, which must be evaluated for each microspecies by using standard statistical methods.[9–12] Finally, the two last products $\prod''$ and $\prod'''$ run over all the pairs of intermetallic (u^{MM}) or interligand (u^{LL}) interactions that occur in the $[M_mL_n]$ microspecies.[12] Obviously, the reliable estimation of these four parameters requires a large amount of independent macroscopic constants that characterize comparable complexation events, a situation which is met when the thermodynamic equilibria relevant to the formation of the bimetallic $[Eu_2(\mathbf{L1})_3]^{6+}$ and $[Eu_2(\mathbf{L2})_3]^{6+}$ and trimetallic $[Eu_3(\mathbf{L3})_3]^{9+}$ triple-stranded helicates are simultaneously considered (only two different tridentate binding units N_2O and N_3 are involved in these complexes; Scheme 1). A complete set of microscopic parameters $f_{N_2O}^{Eu}$, $f_{N_3}^{Eu}$, u^{EuEu}, u^{LL}, and c^{eff} results,[13] and Equation (2) can be then used to predict the stability constant of the unknown tetrametallic homologue $[Eu_4(\mathbf{L4})_3]^{12+}$ [Eq. (3)].

$$\beta_{4,3}^{Eu,L4} = 2\,(f_{N_2O}^{Eu})^6\,(f_{N_3}^{Eu})^6\,(u^{LL})^{12}\,(u^{EuEu})^{4.33}\,(c^{eff})^6 \quad (3)$$

We calculate $\log(\beta_{4,3}^{Eu,L4}) = 42.5$ for the saturated triple-stranded helicate $[Eu_4(\mathbf{L4})_3]^{12+}$ [Eq. (3)], which is much larger than $\log(\beta_{3,3}^{Eu,L4}) = 35.5$, $\log(\beta_{3,2}^{Eu,L4}) = 27.4$, and $\log(\beta_{4,2}^{Eu,L4}) = 31.5$ predicted for its decomposition products, respectively, in excess of ligand ($[Eu_3(\mathbf{L4})_3]^{9+}$) or in excess of metal ($[Eu_3(\mathbf{L4})_2]^{9+}$ and $[Eu_4(\mathbf{L4})_2]^{12+}$; detailed calculations are given in the Supporting Information). The associated predicted distribution curves for a total ligand concentration

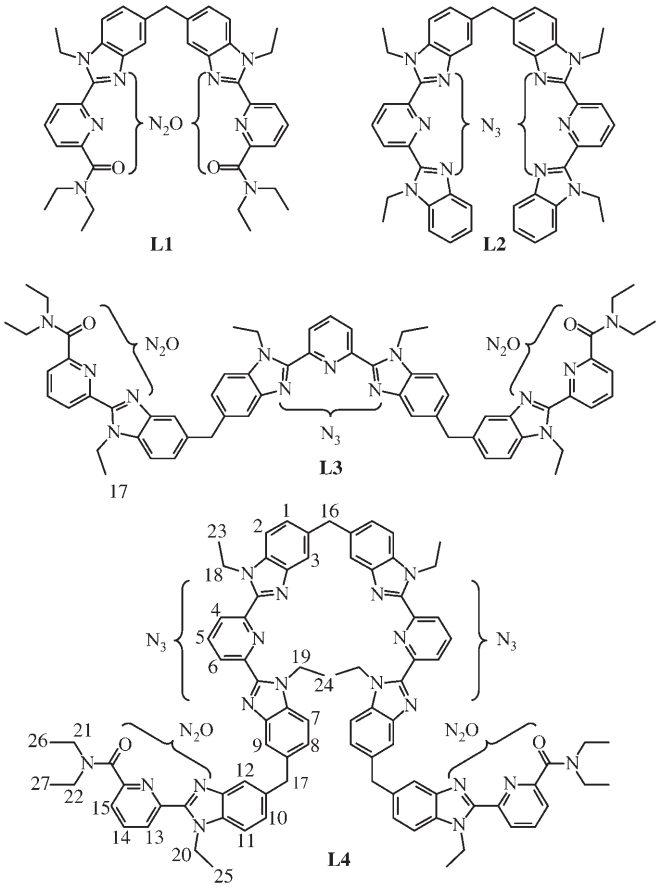

Scheme 1. Structures of the ligands **L1**–**L4**, with the common N_3 and N_2O tridentate binding sites highlighted and the numbering scheme used for the ^{1}H NMR spectroscopic analysis given.

$|\mathbf{L4}|_{tot} = 10^{-3}$ M show that $[Eu_4(\mathbf{L4})_3]^{12+}$ corresponds to > 95% of the solution species for the stoichiometric ratio Eu/**L4** = 1.33, despite its high 12+ charge (see the Supporting Information). With this encouraging prediction in mind, we embarked upon a program to prepare the first stable tetrametallic lanthanide-containing triple-helical complex. Our ultimate goal is concerned with the exploration of the exact dependence of u^{MM} and c^{eff} on the intersite separation d, which is responsible for 1) the potential programming of local intermetallic dielectric constants (through $\Delta E^{MM} \propto 1/\varepsilon_r d$) and 2) the quantitative description of preorganization in self-assembled processes (through $c^{eff} \propto 1/d^n$).[6,11,12] Herein, we present the synthetic strategy, isolation, and structural and thermodynamic characterizations of the first tetrametallic lanthanide triple-stranded helicate $[Eu_4(\mathbf{L4})_3]^{12+}$. Following the original synthetic strategy developed for the preparation of **L3**,[14] we attempt to react the unsymmetrical *o*-nitroaminoarene **3**[14] with the diacid **2** (Scheme 2).[15]

However, **3** proved to be such a poor nucleophile that it does not react with the activated dicarbonyl chloride **2**-$(COCl)_2$ (Scheme 2, left). The remarkable C-shaped molecular structure of **3** observed in the solid state[16] may help to rationalize its poor nucleophilicity because 1) one face of the incriminated secondary ethyl amine N1 is blocked by the distal diethylcarboxamido group bound to the pyridine ring and 2) the H1 proton is involved in an intramolecular hydrogen bond with the adjacent nitro group N1–H1···O1 (N1···O1: 2.634(3) Å, ∢ N1–H1···O1: 130(2)°; Figure 1). Removing the terminal *N*,*N*-diethylcarboxamide pyridyl group in **1** sufficiently improves the nucleophilicity of the secondary amine to react with **2**-$(COCl)_2$ to give the bis(*o*-nitroaminoarene) **4**, which can be further successfully converted into **L4** (Scheme 2, right).

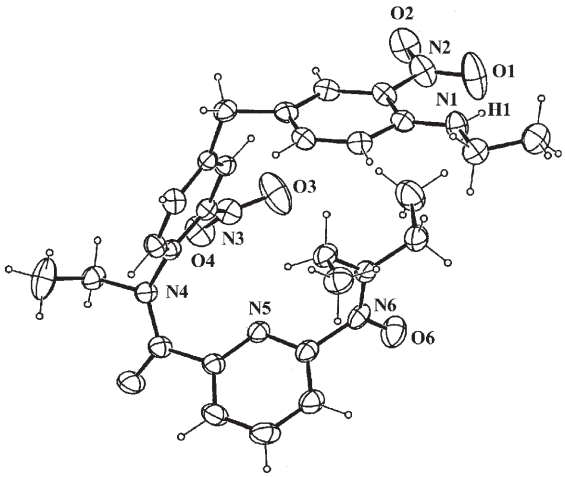

Figure 1. Perspective view of the C-shaped molecular structure of the *o*-nitroaminoarene synthon **3** with partial numbering. Ellipsoids are shown at the 50% probability level.

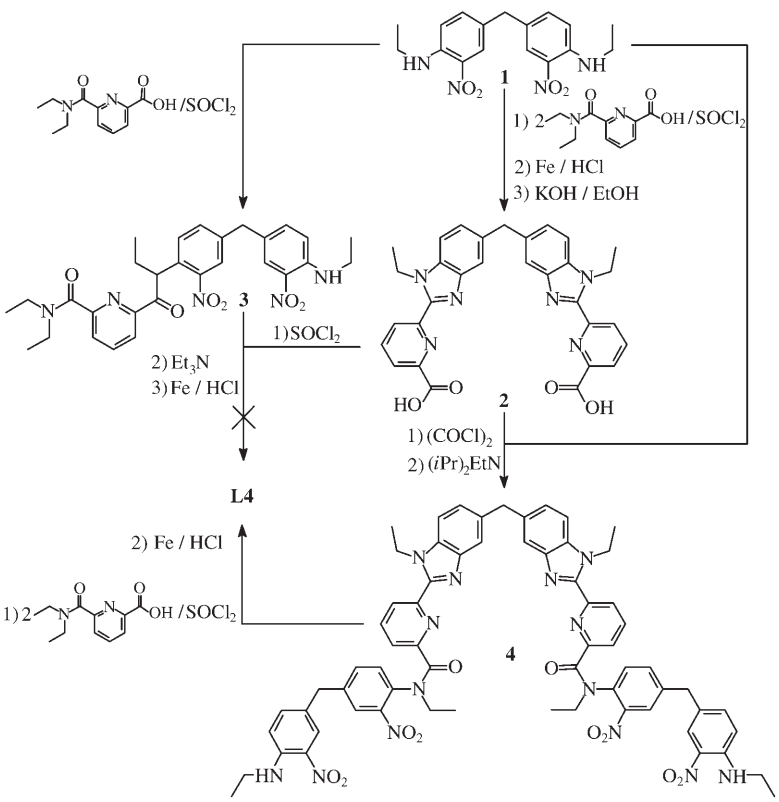

Scheme 2. Synthetic strategy for the preparation of **L4**.

ESI-MS titrations of **L4** (10^{-3} M) with $[Ln(CF_3SO_3)_3]\cdot x H_2O$ ($x = 3$–5) in acetonitrile (Ln = La, Eu, Lu) are dominated by the signals of the saturated species $[Ln_4(\mathbf{L4})_3(CF_3SO_3)_n]^{(12-n)+}$ ($n = 3$–9) together with minor signals (< 10%) that arise from the unsaturated intermediates $[Ln_3(\mathbf{L4})_3(CF_3SO_3)_n]^{(9-n)+}$ (excess of ligand, Ln/**L4** < 1.33) and $[Ln_3(\mathbf{L4})_2(CF_3SO_3)_n]^{(9-n)+}$ and $[Ln_4(\mathbf{L4})_2(CF_3SO_3)_n]^{(12-n)+}$ (excess of metal, Ln/**L4** > 1.33; see the Supporting Information). Parallel ^{1}H NMR titrations in CD_3CN/CD_2Cl_2 (9:1, $|\mathbf{L4}|_{tot} = 8 \times 10^{-3}$ M) confirm this behavior with the stepwise conversion of free **L4** into $[Ln_4(\mathbf{L4})_3]^{12+}$, which largely dominates the speciation in solution (only very weak signals are detected for some low-symmetrical intermediates; see the Supporting Information). The only species detected in solution for Ln/**L4** = 1.33 are $[Ln_4(\mathbf{L4})_3]^{12+}$, and their ^{1}H NMR spectra are compatible with D_3-symmetry (six equivalent half-ligand strands that lead to 15 different CH signals, an enantiotopic central methylene signal for H16,16′, and six diastereotopic methylene protons H17,17′–H22,22′; Figure 2). Finally, preliminary-batch spectrophotometric titrations show complicated variations of the absorption spectra for Eu/**L4** in the range 0.1–4.0 ($|\mathbf{L4}|_{tot} = 10^{-4}$ M, CH_3CN + 5% CH_2Cl_2; see the Supporting Information), which can be satisfyingly fitted with the four absorbing complexes $[Eu_3(\mathbf{L4})_3]^{9+}$, $[Eu_4(\mathbf{L4})_3]^{12+}$, $[Eu_3(\mathbf{L4})_2]^{9+}$, and $[Eu_4(\mathbf{L4})_2]^{12+}$. The associated macroscopic constants $\log(\beta_{3,3}^{Eu,L4}) = 36.2(1.9)$, $\log(\beta_{4,3}^{Eu,L4}) = 42.1(1.9)$, $\log(\beta_{3,2}^{Eu,L4}) = 27.9(1.4)$, and $\log(\beta_{4,2}^{Eu,L4}) = 32.0(1.7)$ match our predictions within experimental errors.

The diffusion of diethyl ether into a concentrated solution of $[Ln_4(\mathbf{L4})_3]^{12+}$ in methanol provides white microcrystals in 70–85% yield; the elemental analyses were shown to be compatible with $[Ln_4(\mathbf{L4})_3](CF_3SO_3)_{12}\cdot x H_2O \cdot y CH_3OH$ (Ln = La: $x = 8.1$,

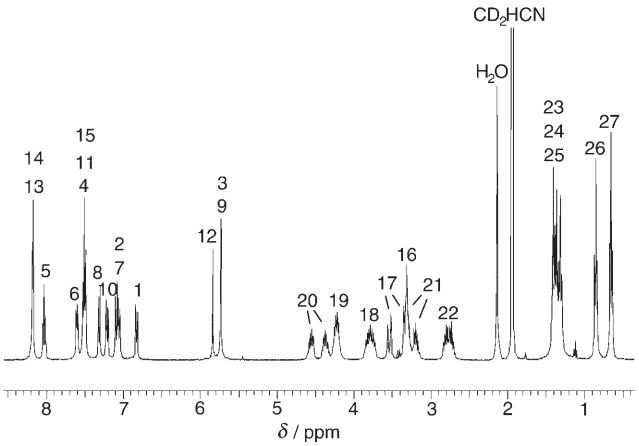

Figure 2. ^{1}H NMR spectrum of the D_3-symmetrical complex $[La_4(\mathbf{L4})_3]^{12+}$ in CD_3CN (298 K, numbering given in Scheme 1).

$y = 1.6$; Ln = Eu: $x = 5.0$, $y = 2.3$; Ln = Lu: $x = 9.6$, $y = 4.7$; see the Supporting Information). Their ESI-MS and ^{1}H NMR spectra obtained after redissolution in acetonitrile are identical with those obtained during the original titration processes (except for an extra peak in the ^{1}H NMR spectrum corresponding to CH_3OH), and slow recrystallization from methanol/diethyl ether gives prisms of $[Eu_4(\mathbf{L4})_3](CF_3SO_3)_{12}\cdot 5\,H_2O\cdot 5\,CH_3OH$ (**5**) suitable for X-ray diffraction studies.[17] The crystal structure of **5** is composed of the expected tetrametallic $[Eu_4(\mathbf{L4})_3]^{12+}$ cations together with 12 non-coordinated triflate anions and 10 interstitial solvent molecules. The pseudo-D_3-symmetrical triple-helical cation $[Eu_4(\mathbf{L4})_3]^{12+}$ shows only minor disorder that affects two peripheral ethyl groups, and its molecular structure (Figure 3a) can be best described as the packing of two terminal $\{EuN_6O_3\}$ and two central $\{EuN_9\}$ pseudo tricapped trigonal prismatic building blocks along the approximate threefold axis defined by the metal ions, as previously reported for $[Eu_3(\mathbf{L3})_3]^{9+}$.[14] The Eu–N and Eu–O bond lengths are standard, as are the bond angles (see the Supporting Information).

The four europium atoms are aligned along the pseudo threefold axis (∢Eu1···Eu2···Eu3: 170.71(1), ∢Eu2···Eu3···Eu4: 172.03(1)°) and regularly spaced by approximately 9.3 Å (Eu1···Eu2: 9.312(1), Eu2···Eu3: 9.054(1), Eu3···Eu4: 9.405(1) Å; Figure 3a). A detailed analysis of the 11 successive helical portions delimited by the 12 parallel facial planes containing the coordinated donor atoms (see Figure 3b and the Supporting Information) shows the usual tightening of the helical pitch about the complexed metal centers, and its relaxation within the intermetallic domains (see the Supporting Information). The total length of the helix amounts to 31 Å (3.1 nm according to modern semantics) for 2.22 turns (Figure 3c), which translates into an average helical pitch of 14.0 Å, comparable with 13.6 Å previously reported for the trimetallic analogous complex $[Eu_3(\mathbf{L3})_3]^{9+}$.[14]

We thus conclude that the incorporation of an additional central tridentate N_3 segment into **L3** to form **L4** is not deleterious for the extension of the helicate series and, in agreement with theoretical thermodynamic predictions, the tetrametallic complex $[Eu_4(\mathbf{L4})_3]^{12+}$ indeed dominates the speciation in solution for concentrations within the millimolar range. Its isolation in the solid state eventually demonstrates the formation of the expected linear triple-stranded helicate. Interestingly, the considerable intermetallic separation in these complexes limits destabilizing intramolecular intercationic repulsions, thus allowing the preparation of stable highly charged polymetallic cations. Although further work is required to address the exact dependence of u^{MM} and c^{eff} on the intersite separation, our novel synthetic strategy for the stepwise extension of the ligand strand offers remarkable perspectives for the design of higher homologues, a crucial

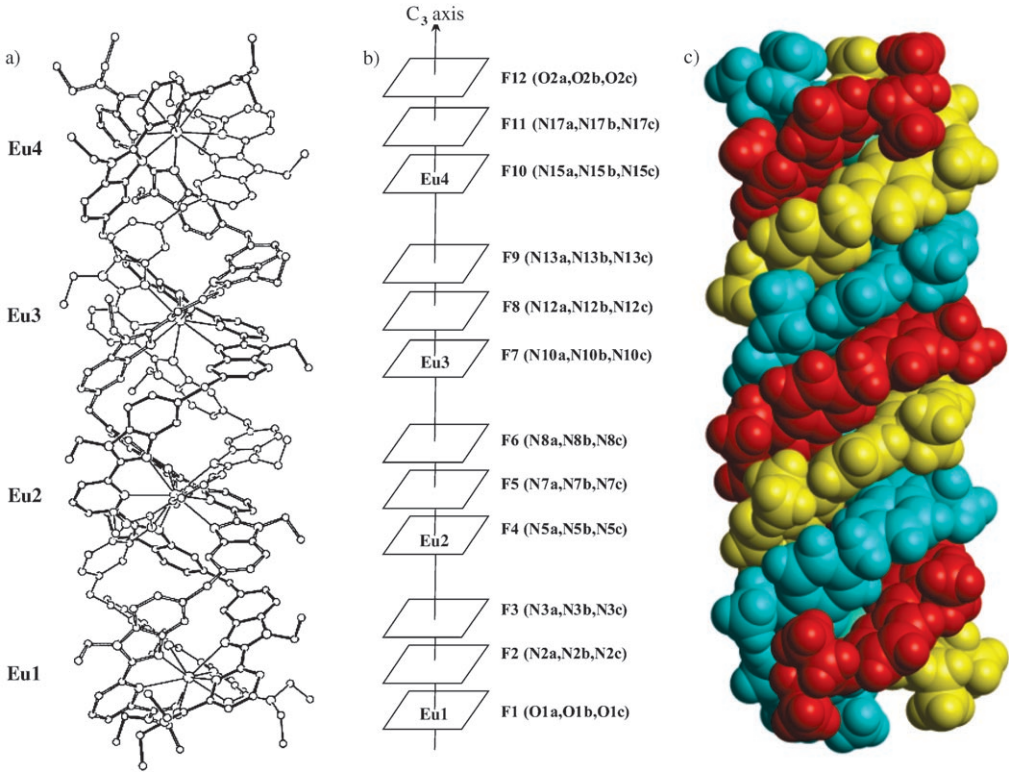

Figure 3. Perspective views of the cation $[Eu_4(\mathbf{L4})_3]^{12+}$ perpendicular to the pseudo threefold axis in the crystal structure of **5**. a) View of the metallic environments (hydrogen atoms have been omitted for clarity); b) schematic representations of the 12 facial planes containing the donor atoms; c) CPK view of the three ligand strands intertwined (represented with different colors).

point for unraveling reliable long-range intermetallic parameters (through u^{MM}) and long-range preorganization effects (through c^{eff}).

Received: August 26, 2005
Published online: November 17, 2005

Keywords: helical structures · lanthanides · polymetallic complexes · self-assembly

[1] a) C. Piguet, G. Bernardinelli, G. Hopfgartner, *Chem. Rev.* **1997**, *97*, 2005; b) M. Albrecht, *Chem. Rev.* **2001**, *101*, 3457; c) M. J. Hannon, L. J. Childs, *Supramol. Chem.* **2004**, *16*, 7.

[2] a) J.-M. Lehn, A. Rigault, *Angew. Chem.* **1988**, *100*, 1121; *Angew. Chem. Int. Ed. Engl.* **1988**, *27*, 1095; b) K. T. Potts, M. Keshavarz-K, F. S. Tham, K. A. Gheysen Raiford, C. Arana, H. D. Abruña, *Inorg. Chem.* **1993**, *32*, 5477; c) A. Marquis-Rigault, A. Dupont-Gervais, A. Van Dorsselaer, J.-M. Lehn, *Chem. Eur. J.* **1996**, *2*, 1395; d) C.-C. Wang, W.-C. Lo, C.-C. Chou, G.-H. Lee, J.-M. Chen, S.-M. Peng, *Inorg. Chem.* **1998**, *37*, 4059; e) R. Krämer, I. O. Fritsky, H. Pritzkow, L. A. Kovbasyuk, *J. Chem. Soc. Dalton Trans.* **2002**, 1307; f) C. J. Matthews, S. T. Onions, G. Morata, L. J. Davis, S. L. Heath, D. J. Price, *Angew. Chem.* **2003**, *115*, 3274; *Angew. Chem. Int. Ed.* **2003**, *42*, 3166.

[3] a) B. R. Serr, K. A. Andersen, C. M. Elliott, O. P. Anderson, *Inorg. Chem.* **1988**, *27*, 4499; b) K. T. Potts, M. Keshavarz-K, F. S. Tham, H. D. Abruña, C. Arana, *Inorg. Chem.* **1993**, *32*, 4422; c) K. T. Potts, M. Keshavarz-K, F. S. Tham, H. D. Abruña, C. Arana, *Inorg. Chem.* **1993**, *32*, 4436; d) K. T. Potts, M. Keshavarz-K, F. S. Tham, H. D. Abruña, C. Arana, *Inorg. Chem.* **1993**, *32*, 4450.

[4] J.-C. G. Bünzli, C. Piguet, *Chem. Rev.* **2002**, *102*, 1897, and references therein.

[5] a) R. Clérac, F. A. Cotton, K. R. Dunbar, C. A. Murillo, I. Pascual, X. Wang, *Inorg. Chem.* **1999**, *38*, 2655; b) J. K. Berra, K. R. Dunbar, *Angew. Chem.* **2002**, *114*, 4633; *Angew. Chem. Int. Ed.* **2002**, *41*, 4453.

[6] a) L. J. Prins, D. N. Reinhoudt, P. Timmerman, *Angew. Chem.* **2001**, *113*, 2446; *Angew. Chem. Int. Ed.* **2001**, *40*, 2382; b) A. Mulder, J. Huskens, D. N. Reinhoudt, *Org. Biomol. Chem.* **2004**, *2*, 3409, and references therein.

[7] For recent reviews, see: a) D. L. Caulder, K. N. Raymond, *Acc. Chem. Res.* **1999**, *32*, 975; b) S. Leininger, B. Olenyuk, P. J. Stang, *Chem. Rev.* **2000**, *100*, 853; c) B. J. Holliday, C. A. Mirkin, *Angew. Chem.* **2001**, *113*, 2076; *Angew. Chem. Int. Ed.* **2001**, *40*, 2022; d) M. Fujita, M. Tominaga, A. Hori, B. Therrien, *Acc. Chem. Res.* **2005**, *38*, 371.

[8] a) T. M. Garrett, U. Koert, J.-M. Lehn, *J. Phys. Org. Chem.* **1992**, *5*, 529; b) A. Pfeil, J.-M. Lehn, *J. Chem. Soc. Chem. Commun.* **1992**, 838.

[9] a) B. Perlmutter-Hayman, *Acc. Chem. Res.* **1986**, *19*, 90; b) M. Borkovec, J. Hamacek, C. Piguet, *Dalton Trans.* **2004**, 4096.

[10] For a recent review, see: C. Piguet, M. Borkovec, J. Hamacek, K. Zeckert, *Coord. Chem. Rev.* **2005**, *249*, 705.

[11] G. Ercolani, *J. Am. Chem. Soc.* **2003**, *125*, 16097.

[12] a) J. Hamacek, M. Borkovec, C. Piguet, *Chem. Eur. J.* **2005**, *11*, 5217; b) J. Hamacek, M. Borkovec, C. Piguet, *Chem. Eur. J.* **2005**, *11*, 5227.

[13] $f^{Eu}_{N_2O} = 5.9$, $f^{Eu}_{N_3} = 5.6$, $\log(u^{EuEu}) = -2.4$, $\log(u^{LL}) = -0.9$, and $\log(c^{eff}) = -0.9$; taken from Table S2 in reference [12b].

[14] S. Floquet, N. Ouali, B. Bocquet, G. Bernardinelli, D. Imbert, J.-C. G. Bünzli, G. Hopfgartner, C. Piguet, *Chem. Eur. J.* **2003**, *9*, 1860.

[15] M. Elhabiri, R. Scopelliti, J.-C. G. Bünzli, C. Piguet, *J. Am. Chem. Soc.* **1999**, *121*, 10747.

[16] Crystal data for **3**: $C_{28}H_{32}N_6O_6$, $M_r = 548.7$, $T = 200$ K, triclinic, $P\bar{1}$, $Z = 2$, $a = 8.1231(7)$, $b = 11.7582(10)$, $c = 15.4242(15)$ Å, $\alpha = 72.580(10)$, $\beta = 77.868(10)$, $\gamma = 89.854(10)°$, $V = 1367.9(2)$ Å^3; 16181 measured reflections, 5504 unique reflections ($R_{int} = 0.065$), $R = 0.039$, $\omega R = 0.038$ for 364 variables and 2764 contributing reflections ($|F_o| > 4\sigma(F_o)$). CCDC-282004 contains the supplementary crystallographic data for this paper. These data can be obtained free of charge from The Cambridge Crystallographic Data Centre via www.ccdc.cam.ac.uk/data_request/cif.

[17] Crystal data for **5**: $Eu_4C_{278}H_{288}N_{54}O_{52}S_{12}F_{36}$, $M_r = 6894.2$, $T = 200$ K, triclinic, $P\bar{1}$, $Z = 2$, $a = 16.9598(9)$, $b = 29.7098(17)$, $c = 34.8898(15)$ Å, $\alpha = 83.449(6)$, $\beta = 88.614(6)$, $\gamma = 88.695(7)°$, $V = 17457(2)$ Å^3; 113988 measured reflections, 50309 unique reflections ($R_{int} = 0.086$), $R = \omega R = 0.085$ for 3719 variables and 23103 contributing reflections ($|F_o| > 3\sigma(F_o)$). CCDC-282005 contains the supplementary crystallographic data for this paper. These data can be obtained free of charge from The Cambridge Crystallographic Data Centre via www.ccdc.cam.ac.uk/data_request/cif.

